Acta Cryst. (1976). B32, 1749

Polyhedral Deformations in Olivine-Type Compounds and the Crystal Structure of Fe_2SiS_4 and Fe_2GeS_4

By H. Vincent and E. F. Bertaut

Laboratoire des Rayons-X, CNRS, B.P. 166, 38042, *Grenoble-Cédex, France*

W. H. Baur

Department of Geological Sciences, University of Illinois, Chicago, Illinois 60680, *U.S.A.*

and R. D. Shannon

Central Research Department, E. I. du Pont de Nemours, Wilmington, Delaware 19898, *U.S.A.*

(*Received* 19 *June* 1975; *accepted* 5 *December* 1975)

Fe_2SiS_4 and Fe_2GeS_4 have the olivine structure with space group *Pnma*. Cell dimensions are $a=12{\cdot}407$ (2), $b=7{\cdot}198(1)$, $c=5{\cdot}812(1)$ Å for Fe_2SiS_4 and $a=12{\cdot}467(2)$, $b=7{\cdot}213(1)$, $c=5{\cdot}902(1)$ Å for Fe_2GeS_4. The crystal structures were refined by least squares to final values of $R=0{\cdot}052$ and 0·044 respectively for Fe_2SiS_4 and Fe_2GeS_4. The distortions of the coordination octahedra and tetrahedra in the sulfide olivines are smaller than in the oxide and fluoride olivines. The distortion indices (relative deviations from the mean) of the edges of the octahedra and tetrahedra in accurately determined olivines are linear functions of the parameter DI(AB) which measures the misfit of the sizes of the octahedra to the tetrahedra. The adjustment stresses between polyhedra of different dimensions are more important contributors to polyhedral deformation than electrostatic forces. A computer simulation of olivines with varied sizes for the octahedral cations supports this interpretation.

Introduction

Compounds of the A_2BX_4 olivine structure-type have been of great interest to mineralogists and crystallographers because of the presence of the mineral olivine in the earth's mantle. Recent structure refinements have provided abundant data on the olivine-type oxides (Hanke, 1965; Smith, Majumdar & Ordway, 1965; Birle, Gibbs, Moore & Smith, 1968; Eysel & Hahn, 1970; Reid & Ringwood, 1970; Moore, 1972; Wenk & Raymond, 1973). At elevated pressures A_2BO_4 olivines transform to the spinel structure. Kamb (1968) provided a detailed discussion of the factors which determine the relative stabilities of the olivine and spinel phases and Syono, Tokonami & Matsui (1971) studied this transition in the transition metal silicates and germanates. Among the factors considered to be important to the stability of the olivine structures are (1) the presence of shared edges shortened to reduce metal–metal repulsion forces and (2) the relative covalence of the A–X bond.

Baur (1972) simulated the structure of Mg_2SiO_4 on a computer and found that metal–metal repulsion was only partially responsible for the edge shortening; a considerable portion of this edge shortening appeared to be caused by misfit between the octahedra and tetrahedra. Because sulfides appeared to have highly covalent A–X bonds in which repulsion effects should be smaller, the olivines Fe_2GeS_4 and Fe_2SiS_4 seemed to be ideal materials to study in order to improve our understanding of the olivine structure and to determine the effect of octahedral and tetrahedral misfit on shared-edge shortening.

Experimental

Fe_2GeS_4 and Fe_2SiS_4 were prepared in vacuum-sealed quartz tubes from pure ground elements mixed in stoichiometric proportions. The samples were slowly heated to 750 °C, maintained at 750 °C for a week, and then cooled slowly. In the case of Fe_2SiS_4, the product was often inhomogeneous; a certain amount of SiS_2 and FeS or Fe_7S_8 was found at the end of the tube. In order to obtain a pure compound the processes of grinding, placing the sample in a tube and heating must be carried out rapidly or in a dry box because SiS_2 hydrolyzes in air. The problem is not so severe for Fe_2GeS_4.

In the case of Fe_2SiS_4 we obtained single crystals by raising the temperature of the sealed tube 5° per hour to 800°; then cooling it slowly back to 400 °C, then raising it slowly again to 900 °C, *etc.* until in the final cycle the maximum temperature was 1100° and the final temperature was 400 °C. In this way brilliant black irregularly shaped crystals of $\frac{1}{2}$ mm length were obtained. In the case of Fe_2GeS_4 we used a fragment of a large monocrystal prepared by Nitsche (1967).

Precession and Weissenberg photographs of Fe_2SiS_4 and Fe_2GeS_4 showed orthorhombic symmetry. The space group extinctions $hk0$ absent when $h=2n+1$ and $0kl$ absent when $k+l=2n+1$ led to the two possible space groups $Pn2_1a$ (C_{2v}^9) and $Pnma$ (D_{2h}^{16}). Since piezoelectricity tests were negative, we chose *Pnma*. The cell dimensions were determined from (1) powder diffraction patterns obtained in a Guinier camera using Fe $K\alpha$ radiation and a KCl standard, and (2) the single-crystal orientation matrix determined using the automatic diffractometer. These two methods led to the same results after refinement by least squares (Table 1).

Table 1. *Unit-cell edges* (Å) *and volumes* (Å^3) *of sulfide olivines*

Standard deviations are given here and in the following tables in parentheses. They correspond to the last significant digits of the values.

	a	*b*	*c*	*V*
Mg_2SiS_4(1)	12·667 (2)	7·409 (1)	5·916 (1)	555·2
Mg_2GeS_4(2)	12·773 (5)	7·435 (2)	6·005 (2)	570·3
Fe_2SiS_4(3)	12·407 (2)	7·198 (1)	5·812 (1)	519·0
Fe_2GeS_4(3)	12·467 (2)	7·213 (1)	5·902 (1)	530·7

(1) Vincent, 1975; (2) Vincent & Perrault, 1971; (3) this work.

In the case of Fe_2SiS_4 a rectangular parallelepiped of dimensions $0{\cdot}19 \times 0{\cdot}12 \times 0{\cdot}07$ mm was used to obtain intensity data. The linear absorption coefficient is 76 cm^{-1} for Mo $K\alpha$ radiation giving a maximum $\mu r = 0{\cdot}72$ and an average $\mu r = 0{\cdot}5$. The absorption corrections were of the same magnitude as the standard deviations of the intensities; the corrections were made assuming a spherical crystal. In the case of Fe_2GeS_4 a sphere of radius 0·10 mm ($\mu r = 1{\cdot}3$) was used for data collection. Using a Hilger–Watts four-circle diffractometer, a total of 857 observed reflections were measured for Fe_2SiS_4 up to a 2θ value of 70°; 1022 observed reflections were measured for Fe_2GeS_4 up to $2\theta = 76°$. Weak reflections for which statistical deviations were as large as the measured values were considered unobserved. The intensities were corrected for Lorentz and polarization factors and for absorption using the X-RAY 70 Program System for X-ray Crystallography (Stewart, Kundell & Baldwin, 1970) on an IBM 360-67 computer.

The refinement was begun using the parameters of Fe_2GeS_4 (Vincent & Perrault, 1971). Scattering factors were taken from Cromer & Waber (1965) with real and imaginary anomalous dispersion terms given by Cromer (1965). In the case of Fe_2GeS_4 the refinement converged rapidly and resulted in an unweighted R of 0·044. The positional parameters and anisotropic temperature factors are listed in Table 2(*a*). Fe_2SiS_4 refined to an R of 0·078. However a systematic disagreement was observed for strong reflections at low angles: in many cases $|F_o|$ was smaller than $|F_c|$ by as much as 40%. Therefore we used the *LINUS* version (Schlemper, Hamilton & LaPlaca, 1971) of the *ORFLS* least-squares program to refine the secondary extinction parameter according to Zachariasen's (1963) formula. After several cycles R fell to 0·052 and agreement of the observed and calculated structure factors was satisfactory for strong reflections. The final positional parameters and anisotropic temperature factors for Fe_2SiS_4 are given in Table 2(*b*). The value of the secondary extinction factor g is $0{\cdot}68 \times 10^{-4}$. The corresponding mean angular dispersion of the crystallites is 8·6 seconds or a corresponding mosaic block size of 4800 Å.*

The structure of Fe_2SiS_4 and Fe_2GeS_4

In the olivine structure, the anions are approximately hexagonally close packed with $\frac{1}{8}$ of the tetrahedral sites occupied by the A cations (Si^{4+} or Ge^{4+}) and $\frac{1}{2}$ of the octahedral sites occupied by the B cations (Fe^{2+}). The B(1) octahedra are located at a center of symmetry and form infinite edge-shared chains parallel to [010]. In alternating positions to the left and right of the chains and situated half way between two B(1) octahedra, the B(2) octahedra are straddling the mirror planes perpendicular to [010].

The sulfide ion common to the two octahedra B(1)

Table 2. *Positional parameters and thermal parameters* (Å^2) *multiplied by* 10^4 (*except the fractions*)

(*a*) Fe_2GeS_4

	Equi-point	*x*	*y*	*z*	u_{11}	u_{22}	u_{33}	u_{12}	u_{13}	u_{23}
S(1)	4(*c*)	4076 (2)	$\frac{1}{4}$	7113 (4)	84 (9)	93 (9)	73 (9)		5 (8)	
S(2)	4(*c*)	5729 (2)	$\frac{1}{4}$	2441 (4)	60 (8)	108 (9)	98 (9)		2 (8)	
S(3)	8(*d*)	3325 (1)	99 (2)	2520 (3)	92 (6)	97 (6)	89 (6)	−21 (6)	2 (5)	−20 (6)
Ge	4(*c*)	4110 (1)	$\frac{1}{4}$	832 (2)	62 (4)	79 (4)	58 (4)		3 (4)	
Fe(1)	4(*a*)	0	0	0	92 (6)	97 (6)	92 (6)	12 (5)	0 (5)	−5 (6)
Fe(2)	4(*c*)	2294 (1)	$\frac{1}{4}$	5067 (3)	69 (6)	105 (6)	103 (6)		−3 (5)	

(*b*) Fe_2SiS_4

	Equi-point	*x*	*y*	*z*	u_{11}	u_{22}	u_{33}	u_{12}	u_{13}	u_{23}
S(1)	4(*c*)	4079 (2)	$\frac{1}{4}$	7284 (3)	105 (7)	118 (8)	72 (7)		4 (7)	
S(2)	4(*c*)	5692 (1)	$\frac{1}{4}$	2383 (3)	71 (6)	118 (7)	96 (7)		−10 (6)	
S(3)	8(*d*)	3335 (1)	173 (5)	2487 (2)	94 (5)	108 (5)	92 (5)	−18 (4)	5 (4)	1 (4)
Si	4(*c*)	4111 (2)	$\frac{1}{4}$	916 (4)	64 (7)	86 (8)	55 (8)		−5 (8)	
Fe(1)	4(*a*)	0	0	0	107 (5)	123 (5)	109 (5)	−2 (4)	−5 (4)	−13 (4)
Fe(2)	4(*c*)	2299 (1)	$\frac{1}{4}$	5098 (2)	92 (5)	122 (5)	104 (5)		0 (4)	

---

* A list of structure factors has been deposited with the British Library Lending Division as Supplementary Publication No. 31554 (11 pp., 1 microfiche). Copies may be obtained through The Executive Secretary, International Union of Crystallography, 13 White Friars, Chester CH1 1NZ, England.

and the B(2) octahedron forms one of the apices of an occupied A tetrahedron; the other 3 apices are located in a horizontal plane and are provided by 3 sulfide ions of the chain below or above (related by a translation of $+c$ or $-c$). The tetrahedra link the chains in [001]. Each B(1) octahedron shares: 2 edges with 2 B(1) octahedra, 2 edges with 2 B(2) octahedra, 2 edges with 2 A tetrahedra; while each B(2) octahedron shares: 2 edges with 2 B(1) octahedra, 1 edge with 1 A tetrahedron. Table 3 gives the pertinent interatomic distances and angles in Fe_2GeS_4 and Fe_2SiS_4. The mean Si–S distance in Fe_2SiS_4 of 2·130 Å agrees well with the values from $Na_4Si_4S_{10}$, 2·120 Å (Ribes, Olivier-Fourcade, Philippot & Maurin, 1973) and SiS_2, 2·130 Å (Prewitt & Young, 1965). The mean Ge–S distance of 2·222 Å agrees well with the values from $Na_4Ge_4S_{10}$ (2·203 Å), $Ba_2Ge_4S_{10}$ (2·202 Å; Ribes *et al.*, 1973), GeS_2 (2·212 Å; Prewitt & Young, 1965), $GePb_2S_4$ (2·20 Å; Susa & Steinfink, 1971*a*) and $GeCd_4S_6$ (2·20 Å; Susa & Steinfink, 1971*b*).

The polyhedra in the sulfides are considerably less distorted than in the olivine-type oxides. The tetrahedra are almost regular, 3 distances practically equal (2·138 Å for Fe_2SiS_4, 2·227 Å for Fe_2GeS_4) and a 4th slightly shorter (2·111 Å and 2·195 Å, respectively). The three long distances correspond to three sulfur atoms belonging to the three edges shared with the tetrahedron. It is similar for the Fe(2) octahedron where the distances to the three apices of the face containing the shared edges are longer than the other three: 2·600 (×2) and 2·548 compared with 2·500 (×2) and 2·461 Å for Fe_2SiS_4, and 2·629 (×2) and 2·529 compared with 2·491 (×2) and 2·449 Å for Fe_2GeS_4. In the Fe(1) octahedron the Fe–S distances range from 2·508 to 2·533 Å for Fe_2SiS_4 and 2·477 to 2·551 Å for Fe_2GeS_4; in this octahedron all six apices belong to shared edges. The movement or 'recoil' of the cations away from the shared edges has already been observed in numerous olivine-type compounds (Hanke, 1965; Kamb, 1968) and is attributed to the electrostatic repulsion between cations occupying the adjacent polyhedra.

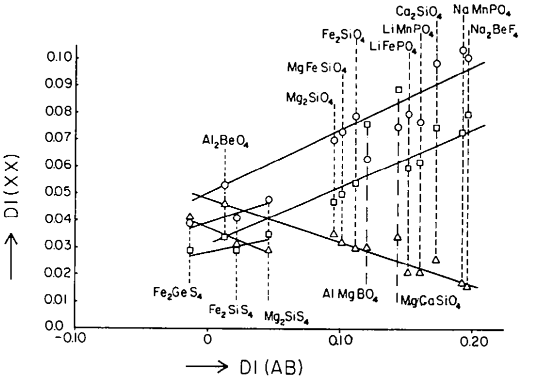

Fig. 1. Polyhedral deformation, DI(XX), in olivine-type compounds *versus* the relative size difference of the octahedra and tetrahedra, DI(AB). For definitions see text. (○ represents a B(1) octahedron, □ represents a B(2) octahedron and △ an A tetrahedron.)

The mean distances Fe(1)–S of 2·517 (Fe_2SiS_4) and 2·517 Å (Fe_2GeS_4) and Fe(2)–S of 2·535 and 2·536 Å are considerably shorter than one would predict on the basis of ionic radii: 0·78 + 1·84 = 2·62 Å (Shannon & Prewitt, 1969, 1970; Pauling, 1960). In the case of Fe_2SiO_4 the observed (Fe–O) distances (Birle, Gibbs,

Table 3. *Bond distances* (Å) *and angles* (°)

Estimated standard deviations are on the average 0·002 Å for cation–sulfur and cation–cation distances, 0·003 Å for sulfur–sulfur distances and 0·1° for angles. Asterisks signify shared edges.

		Fe_2GeS_4	Fe_2SiS_4
(*a*) Tetrahedra			
A–S(1)		2·195	2·111
A–S(3)	(2×)	2·225	2·137
A–S(2)		2·231	2·139
S(1)–A–S(3)	(2×)	116·1	114·8
S(1)–A–S(2)		116·3	114·6
S(3)–A–S(3)*		102·2	103·2
S(3)–A–S(2)*	(2×)	102·0	104·1
S(1)–S(3)	(2×)	3·750	3·578
S(1)–S(2)		3·760	3·576
S(3)–S(3)*		3·464	3·350
S(3)–S(2)*	(2×)	3·462	3·371
Mean S–S		3·608	3·471
(*b*) Octahedra			
Fe(1)–S(1)	(2×)	2·477	2·511
Fe(1)–S(2)	(2×)	2·522	2·508
Fe(1)–S(3)	(2×)	2·551	2·533
S(1)–Fe(1)–S(2)*	(2×)	87·1	87·8
S(1)–Fe(1)–S(2)	(2×)	92·9	92·2
S(1)–Fe(1)–S(3)*	(2×)	83·6	84·2
S(1)–Fe(1)–S(3)	(2×)	96·4	95·8
S(2)–Fe(1)–S(3)*	(2×)	86·1	83·9
S(2)–Fe(1)–S(3)	(2×)	93·9	96·1
S(1)–S(2)*	(2×)	3·442	3·481
S(1)–S(2)	(2×)	3·624	3·615
S(1)–S(3)*	(2×)	3·350	3·381
S(1)–S(3)	(2×)	3·750	3·743
S(2)–S(3)*	(2×)	3·462	3·371
S(2)–S(3)	(2×)	3·708	3·748
Mean S–S		3·556	3·557
Fe(2)–S(2)		2·449	2·461
Fe(2)–S(3)	(2×)	2·491	2·500
Fe(2)–S(1)		2·529	2·548
Fe(2)–S(3)	(2×)	2·629	2·600
S(2)–Fe(2)–S(3)	(2×)	96·0	94·0
S(2)–Fe(2)–S(3)	(2×)	92·5	93·4
S(3)–Fe(2)–S(3)		97·6	100·7
S(3)–Fe(2)–S(1)	(2×)	89·7	89·8
S(3)–Fe(2)–S(3)	(2×)	89·3	89·1
S(1)–Fe(2)–S(3)*	(2×)	81·0	82·1
S(3)–Fe(2)–S(3)*		82·4	80·2
S(2)–Fe(2)–S(1)		171·3	174·0
S(3)–Fe(2)–S(3)	(2×)	168·4	167·3
S(2)–S(3)	(2×)	3·671	3·629
S(2)–S(3)	(2×)	3·671	3·683
S(3)–S(3)		3·749	3·848
S(3)–S(1)	(2×)	3·540	3·562
S(3)–S(3)	(2×)	3·600	3·578
S(1)–S(3)*	(2×)	3·350	3·381
S(3)–S(3)*		3·464	3·350
Mean S–S		3·573	3·572

Moore & Smith, 1968) are respectively 2·159 and 2·178 Å in good agreement with the sum of the radii, 0·78+1·38=2·16 Å. We believe this difference in the case of the sulfides to be caused by the largely covalent nature of the Fe–S bond. Another anomaly can be observed when comparing the cell dimensions of Fe_2GeS_4 and Mg_2GeS_4 (Table 1). The cell volume of Fe_2GeS_4 is smaller than that of Mg_2GeS_4; this is not consistent with the fact that the cell volumes of FeO and Fe_2SiO_4 are larger than those of MgO and Mg_2SiO_4. This was discussed in a general study of compounds containing the transition metals Mn, Fe, Co, Ni and anions with differing electronegativities such as F, Cl, Br, I, O, S, and Se. For all these compounds a lattice contraction is observed relative to the magnesium-containing isomorphous compounds. This contraction increases as a function of the degree of covalence of the metal–ligand bonds (Shannon & Vincent, 1974).

In both Fe_2SiS_4 and Fe_2GeS_4 the shared edges are considerably shorter than the unshared edges. According to a corollary to Pauling's third rule shortening of shared edges is an indication of the ionicity of bonds in a solid (Pauling, 1960). In Fe_2SiS_4 the difference between the average of the shared edges and the average of non-shared edges (Table 4) is 6 % for the tetrahedron and 9 % for the Fe(1) and 8 % for the Fe(2) octahedra; in Fe_2GeS_4 these same differences are 8 %, 8 % and 7 % respectively. By comparison, these differences for Fe_2SiO_4 are 6 %, 17 % and 11 %, respectively. One notices that although the deformation of tetrahedra is similar, that of the octahedra is considerably smaller in the sulfides. To the extent that the deformation of the polyhedra is due to the electrostatic repulsion of the cations, this seems normal because (1) the cation–cation distances are clearly larger in Fe_2SiS_4 (Fe–Si minimum = 3·176 Å) than in Fe_2SiO_4 (2·785 Å) and (2) the Fe–S bonds are more covalent than Fe–O bonds. The covalent character is apparent in the magnetic properties of these compounds; their Néel temperatures (127°K for Fe_2SiS_4, 146K for Fe_2GeS_4) are much higher than that of Fe_2SiO_4 (62K) (Kondo & Miyahara, 1966). This corresponds to much stronger Heisenberg–Néel exchange integrals, and hence a greater orbital overlap of iron and sulfur than iron and oxygen. In order to interpret the antiferromagnetic structure of Fe_2GeS_4 at low temperature, Vincent & Bertaut (1973*a*) assumed negative and strong Fe(2)–S–Fe(1) super-exchange. The reduction of the spin (10 %) found on the Fe(2) sites reveals a significant hybridization of the t_{2g} orbitals of Fe(2) with the *p* orbitals of the sulfur ions.

Polyhedral deformations in the olivine structure

Up to now we have discussed the polyhedral deformation by assuming that Pauling's third rule is valid and

Table 4. *Mean interatomic distances* (Å) *and polyhedral distortions in olivine-type compounds*

All DI are multiplied by 10^3. Asterisks signify shared edges.

	Mean A–X	Mean B(1)–X	Mean B(2)–X	Mean shared and non-shared edges around			DI (AB)	DI (XX)		
				A	B(1)	B(2)		A	B(1)	B(2)
Na_2BeF_4(*a*)	1·551	2·300	2·331	2·490*	2·902*	2·910*	196	16	101	80
				2·570	3·552	3·398				
Al_2BeO_4(*b*)	1·632	1·890	1·937	2·523*	2·528*	2·535*	13	46	53	34
				2·768	2·810	2·789				
$AlMgBO_4$(*c*)	1·489	1·900	2·094	2·349*	2·512*	2·556*	120	30	63	76
				2·493	2·851	3·064				
$MgCaSiO_4$(*d*)	1·626	2·131	2·370	2·556*	2·778*	2·883*	143	34	75	89
				2·737	3·229	3·479				
Mg_2SiO_4(*e*)	1·635	2·103	2·135	2·566*	2·756*	2·766*	95	35	70	47
				2·752	3·171	3·080				
Fe_2SiO_4(*e*)	1·637	2·159	2·178	2·586*	2·805*	2·823*	111	30	78	54
				2·745	3·277	3·136				
$MgFeSiO_4$(*e*)	1·639	2·129	2·155	2·583*	2·780*	2·795*	101	32	73	50
				2·755	3·219	3·103				
Ca_2SiO_4(*f*)	1·646	2·352	2·392	2·611*	2·974*	2·978*	172	26	99	75
				2·753	3·629	3·489				
$LiFePO_4$(*g*)	1·544	2·154	2·163	2·466*	2·788*	2·751*	151	21	80	60
				2·571	3·272	3·129				
$LiMnPO_4$(*h*)	1·542	2·165	2·201	2·463*	2·813*	2·774*	160	21	77	62
				2·568	3·282	3·192				
$NaMnPO_4$(*i*)	1·546	2·374	2·211	2·478*	2·986*	2·904*	192	17	104	73
				2·563	3·662	3·189				
Mg_2SiS_4(*j*)	2·126	2·584	2·607	3·360*	3·474*	3·436*	46	29	48	35
				3·564	3·823	3·755				
Fe_2SiS_4(*k*)	2·131	2·517	2·535	3·364*	3·411*	3·371*	22	31	41	29
				3·577	3·702	3·639				
Fe_2GeS_4(*k*)	2·219	2·517	2·536	3·463*	3·418*	3·388*	−13	41	39	29
				3·753	3·694	3·635				

(*a*) Hanke, 1965; (*b*) Farrell, Fang & Newnham, 1963; (*c*) Fang & Newnham, 1965; (*d*) Onken, 1965; (*e*) Birle *et al.*, 1968; (*f*) Czaya, 1971; (*g*) Finger & Rapp, 1970; (*h*) Geller & Durand, 1960; (*i*) Moore, 1972; (*j*) Vincent, 1975; (*k*) this work.

that electrostatic repulsion is the main factor in shortening shared edges. However, Baur (1972) suggested that shared-edge shortening in olivines is due only partly to metal–metal repulsion forces. He attributed in Mg_2SiO_4 approximately $\frac{1}{3}$ of octahedral edge shortening and $\frac{1}{2}$ of tetrahedral edge shortening to repulsive forces and the remainder to 'adjustment stresses' which arise because of shared edges between polyhedra of very different dimensions.

In order to see if this idea is consistent with the polyhedral deformation in other olivines, we have plotted in Fig. 1 for all precisely determined olivine structures the distortion parameters DI(XX) of the B(1) and B(2) octahedra and the A tetrahedra *versus* a parameter DI(AB) which defines the size difference between the octahedra and the tetrahedron. Using the notation of Baur (1974) we define:

$$\mathrm{DI(XX)} = \sum_{i}^{n} |\mathrm{XX}_i - \mathrm{XX}_m| / n\mathrm{XX}_m\,,$$

where XX_i is the length of the edge i of the polyhedron formed by the anions X, $\mathrm{XX}_m = \langle \mathrm{X} - \mathrm{X} \rangle$ of the polyhedron, n = number of edges in the polyhedron and

$$\mathrm{DI(AB)} = (|\mathrm{BX}_m - \mathrm{AX}_m| / \mathrm{BX}_m) - 0{\cdot}134\,,$$

where $\mathrm{BX}_m = [\langle \mathrm{B(1)} - \mathrm{X} \rangle + \langle \mathrm{B(2)} - \mathrm{X} \rangle]/2$ and $\mathrm{AX}_m = \langle \mathrm{A} - \mathrm{X} \rangle$.

As Table 4 and Fig. 1 show, DI(XX) seems to vary linearly with DI(AB). This is qualitatively consistent with Baur's findings. The deformation of B(1) and B(2) octahedra increases regularly with the size difference between octahedra and tetrahedra for a given anion and the slopes of the lines are similar for both B sites. The B(1) and B(2) points corresponding to $AlMgBO_4$ and $MgCaSiO_4$ are inverted. Obviously the relationship is disturbed when the B(2) cation is considerably larger (0·2 Å). However, it is not disturbed by the fact that of the 14 compounds entered in Table 4 and Fig. 1 eight are of the $B_2^{2+}A^{4+}X_4^{2-}$ type, while three are examples of $B(1)^{+}B(2)^{2+}A^{5+}X_4^{2-}$, and one each of $B_2^{3+}A^{2+}X_4^{2-}$, $B_2^{1+}A^{2+}X_4^{1-}$ and $B(1)^{3+}B(2)^{2+}A^{3+}X_4^{2-}$. The fact that the relationship holds for widely different formal charges, but not for the case of the B(2) cation larger than the B(1) cation shows that the distortions are more influenced by the misfit between the dimensions of the polyhedra than by electrostatic repulsion forces. The greater distortion of the B(1) sites compared with that of the B(2) sites is related to the fact that B(1) has a total of 6 shared edges while the B(2) site has only 3 shared edges.

The deformation of the tetrahedra varies in the opposite sense; it diminishes linearly with DI(AB). This was not anticipated. Kamb (1968) showed that in the olivine structure the shortening of the tetrahedral shared edges is accompanied by shortening of the octahedral shared edges. From this he concluded that this mechanism favors the olivine structure over the spinel structure. This reasoning based on Pauling's third rule, which considers only the electrostatic interaction forces, implies that the deformation of octahedra and tetrahedra are parallel and cumulative. However, Fig. 1 shows that they are not. The shortening of the edges shared by the octahedra tends to flatten the B(1) octahedron within the plane (001) with increasing size of the B(1) cation and causes an elongation of all the edges which are parallel to the (001) plane, including those which are shared with the tetrahedra. Thus we see in Table 4 that for Mg_2SiO_4, Fe_2SiO_4 and γCa_2SiO_4 in the Si tetrahedra the mean value of the shared edges increases (2·566, 2·586, 2·611 Å) while the mean value of the unshared edges remains constant (2·752, 2·745, 2·753 Å). In other words, the shortening of the edges shared by octahedra opposes and limits the shortening of the edges shared with the tetrahedra.

For the sulfides, Fe_2SiS_4, Fe_2GeS_4 and Mg_2SiS_4 (Vincent, 1975) the difference between the mean size of octahedra and tetrahedra is smaller than for all the oxides except Al_2BeO_4. The polyhedra in the sulfides are less deformed for a given value of DI(AB) compared with the oxides since the lines for the different sites are shifted towards lower DI(XX) values. This indicates that the packing of the sulfur atoms is more regular than that of the oxygen atoms and tends toward ideal hexagonal close packing. Note that in the ideal case one has $\mathrm{A} - \mathrm{X}_i / \mathrm{B} - \mathrm{X}_i = \sqrt{3}/2$ for any i. In this case one should observe for $\mathrm{DI(AB)} = 1 - \sqrt{3}/2 - 0{\cdot}134 = 0$, a value $\mathrm{DI(XX)} = 0$, for all the polyhedra of the structure. This is obviously not the case (Fig. 1) for the known olivines where the shortening of the shared edges stabilizes the structure. The absolute values of the differences in the shared and unshared edges are about the same for the sulfides and for Al_2BeO_4. However, the cation–anion bond lengths are longer, therefore the relative distortions [DI(XX)] are smaller for the sulfides. This may reflect the smaller degree of influence of electrostatic forces in the sulfides compared with the oxides. Since in the sulfides the cation–cation distances are longer, the electrostatic repulsions are less and the distortion indices tend more towards the ideal case of $\mathrm{DI(XX)} = 0$ at $\mathrm{DI(AB)} = 0$.

The notion of polyhedral deformations being largely caused by geometric adjustments can be tested by the computer simulation (Baur, 1972) of olivines with varying lengths of the B–O distances. Computer simulation of crystal structures can be performed when the number of predicted interatomic distances exceeds the number of parameters necessary to define the structure. The predicted distances are then used as observations in a least-squares refinement (Meier & Villiger, 1969). We simulated the crystal structures of hypothetical B_2SiO_4 olivines assuming B–O distances ranging from 1·693 to 2·493 Å, in steps of 0·1 Å. The Si–O distances were kept constant at 1·639 Å. The difference between the lengths of the shared and unshared tetrahedral edges was taken as 0·29 Å (for the simulation with B–O of 1·693 Å) and linearly reduced to 0·05 Å (for B–O of 2·493 Å). This was done in order to account for the different degrees of distortion of the tetrahedral group expected to occur with different sizes of the B ion. The distortion of the octahedron due to shared edges was assumed to result in a constant difference of 0·15 Å between the lengths of the shared and unshared edges. The weights given to the B–O and Si–O distances in the distance least-squares refinement were the electrostatic bond strengths. For O–O the weights were taken uniformly as 0·07 (Baur, 1972). It should be emphasized that the simulated structure is of the $B_2^{2+}A^{4+}X_4^{2-}$ type. The calculated distortions of the simulated B_2SiO_4 olivines (Fig. 2) follow closely the trend observed for the actual olivines entered in Fig. 1. For large values of DI(AB), that is long B–O distances, the absolute values of the calculated and the observed distortion indices are similar. Towards smaller DI(AB) values the relative positions of the calculated DI(XX) values for B(1), B(2) and A remain correct but their absolute values are smaller than for the observed DI(XX). This must be interpreted to mean that for smaller B–O distances the observed distortions have an additional component which is not contained in the simulation model. Most likely this is electrostatic repulsion which is not explicitly provided for in the simulation. The simulation of the sulfide olivines was done in an analogous fashion. The shapes of the DI(XX) *versus* DI(AB) curves are the same as for B_2SiO_4, however, they are displaced compared to those for B_2SiO_4 in the same way as they are in Fig. 1.

In order to test the dependence of the DI(XX) on electrostatic repulsions we plotted the distortion indices of A against the distances A–B(1) and A–B(2); the DI(XX) of B(1) against B(1)–B(1), B(1)–B(2) and B(1)–A; and DI(XX) of B(2) against B(2)–B(1) and B(2)–A. The best linear dependence was observed for DI(XX) of B(1) *versus* B(1)–A, while the plots involving DI(XX) of A resulted in meaningless scatter. As a whole these relationship do not match the simplicity of Fig. 1. Recently Fleet (1974) has argued that polyhedral distortions in olivines, clinopyroxenes and amphiboles are correlated with the electrostatic potentials at the cation sites. However, he found that in contradiction to his expectations the Fe_2SiO_4 olivine has more distorted octahedra than the Mg_2SiO_4 olivine. This contradiction can be easily resolved when we take into account the larger size of the FeO_6 octahedra as compared with the MgO_6 octahedra and when we view the distortions as a consequence of size effects. This interpretation is supported by the fact that in Fe_2SiS_4 the octahedra are less distorted than in Mg_2SiS_4, because the FeS_6 octahedra are *smaller* than the MgS_6 octahedra (see Table 4).

However, it could also be argued that in the two oxides the ionicities of the bonds and the repulsion forces are similar. Because the Fe^{2+} ion ($3d^6$) is less symmetrical than the Mg^{2+} ion ($2p^6$), the Fe octahedron is more deformed than that of Mg. In the two sulfides the metal–sulfur bonds have a more covalent character for Fe_2SiS_4 than for Mg_2SiS_4 (Vincent & Bertaut, 1973*b*); the repulsion forces are therefore weaker in the first compound and although the sulfur ions are certainly more sensitive than the oxygens to the electronic asymmetry of the cations because of greater hybridization of the metal and ligand orbitals, the deformation of Fe octahedra is smaller than that of Mg. However, these two interpretations are not necessarily completely independent because the repulsion forces as well as the cation size are both functions of the degree of covalence of the metal–ligand bonds (Shannon & Vincent, 1974). Because Fe_2SiS_4 is more covalent than Mg_2SiS_4, the repulsion forces of the octahedra are weaker in Fe_2SiS_4 and $\langle Fe–S\rangle$ (2·525 Å) is smaller than $\langle Mg–S\rangle$ (2·596 Å).

Stability of Fe_2GeS_4

Characteristic of the olivine structure are small tetrahedral ions on the one hand and relatively large octahedral ions on the other. The spinel structure is stable for relatively small octahedral ions and large tetrahedral ions (Kamb, 1968). Hence a compound may have the olivine structure if the ratio $d_B/d_A=\langle B-X\rangle/\langle A-X\rangle$ is larger than a certain limiting value, and spinel if it is smaller. Its theoretical limiting value is that which corresponds to close packing of spheres, *i.e.* $d_B/d_A=2/\sqrt{3}=1\cdot155$ (a value independent of the sphere radius). Kamb has shown that in the oxides this limit is always higher than this theoretical value ($d_B/d_A=1\cdot18$–$1\cdot22$). This value apparently increases as the charge on the A cation and as the covalence of the B–O bond increase. The sulfides discussed in this paper are distinguished by d_B/d_A values very close to the limiting value $2\sqrt{3}=1\cdot155$; Fe_2GeS_4 has a clearly lower ratio $d_B/d_A=1\cdot138$. If one considers that the Fe–S bonds have a distinctly covalent character, Fe_2GeS_4 should have a spinel structure. Therefore, we subjected Fe_2GeS_4 to elevated pressure. At 40 kbar and 800 °C the olivine structure remained stable; at 80 kbar and 800 °C a decomposition was observed with FeS_2 pyrite formation, but no trace of spinel was found.

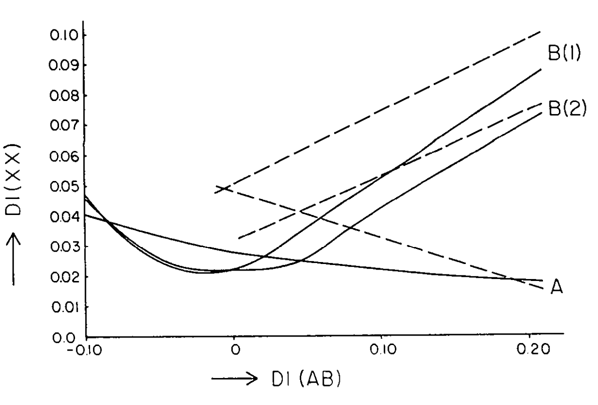

Fig. 2. Calculated and observed polyhedral deformation *versus* DI(AB) for olivines. Solid lines are calculated and dashed lines are experimental.

Hence, it seems that the stability relations of the olivine and spinel structures established by Kamb for oxides do not apply to the sulfides.

We thank R. Nitsche for the Fe_2GeS_4 crystals, B. Fouilleux and A. Durif for help and advice in the data collection, D. Tranqui and I. Tordjman for the structure refinement programs, and the Computer Center of the University of Illinois, Chicago for computer time.

References

BAUR, W. H. (1972). *Amer. Min.* **57**, 709–731.

BAUR, W. H. (1974). *Acta Cryst.* B**30**, 1195–1215.

BIRLE, J. E., GIBBS, G. V., MOORE, P. B. & SMITH, J. V. (1968). *Amer. Min.* **53**, 807–824.

CROMER, D. T. (1965). *Acta Cryst.* **18**, 17–23.

CROMER, D. T. & WABER, J. T. (1965). *Acta Cryst.* **18**, 104–109.

CZAYA, R. (1971). *Acta Cryst.* B**27**, 848–849.

EYSEL, W. & HAHN, T. (1970). *Z. Kristallogr.* **131**, 322–341.

FANG, J. H. & NEWNHAM, R. (1965). *Miner. Mag.* **35**, 196–199.

FARRELL, E. F., FANG, J. H. & NEWNHAM, R. (1963). *Amer. Min.* **48**, 804–810.

FINGER, L. W. & RAPP, G. R. (1970). *Carnegie Inst. Wash. Yearb.* **68**, 290–292.

FLEET, M. E. (1974). *Amer. Min.* **59**, 1083–1093.

GELLER, S. & DURAND, J. L. (1960). *Acta Cryst.* **13**, 325–331.

HANKE, K. (1965). *Beitr. Mineral. Petrogr.* **11**, 535–558.

KAMB, B. (1968). *Amer. Min.* **53**, 1439–1455.

KONDO, H. & MIYAHARA, S. (1966). *J. Phys. Soc. Japan*, **21**, 2193–2196.

MEIER, W. M. & VILLIGER, H. (1969). *Z. Kristallogr.* **129**, 411–423.

MOORE, P. B. (1972). *Amer. Min.* **57**, 1333–1344.

NITSCHE, R. (1967). *Fortschr. Mineral.* **44**, (2), 231–287.

ONKEN, (1965). *Mineral. Petrogr. Mitt.* **10**, 34–44.

PAULING, L. (1960). *The Nature of the Chemical Bond*, 3rd ed. Ithaca: Cornell Univ. Press.

PREWITT, C. T. & YOUNG, H. S. (1965). *Science*, **149**, 535–537.

REID, A. F. & RINGWOOD, A. E. (1970). *J. Solid State Chem.* **1**, 557–565.

RIBES, M., OLIVIER-FOURCADE, J., PHILIPPOT, E. & MAURIN, M. (1973). *J. Solid State Chem.* **8**, 195–205.

SCHLEMPER, E. O., HAMILTON, W. C. & LAPLACA, S. J. (1971). *J. Chem. Phys.* **54**, 3990–4000.

SHANNON, R. D. & PREWITT, C. T. (1969). *Acta Cryst.* B**25**, 925–946.

SHANNON, R. D. & PREWITT, C. T. (1970). *Acta Cryst.* B**26**, 1046–1048.

SHANNON, R. D. & VINCENT, H. (1974). *Struct. Bond.* **19**, 1–43.

SMITH, D. K., MAJUMDAR, A. & ORDWAY, F. (1965). *Acta Cryst.* **18**, 787–795.

STEWART, J. M., KUNDELL, F. A. & BALDWIN, T. C. (1970). The X-RAY 70 system. Computer Science Center, Univ. of Maryland, College Park, Maryland.

SUSA, K. & STEINFINK, H. (1971*a*). *J. Solid State Chem.* **3**, 75–82.

SUSA, K. & STEINFINK, H. (1971*b*). *Inorg. Chem.* **10**, 1754–1756.

SYONO, Y., TOKONAMI, M. & MATSUI, Y. (1971). *Phys. Earth Planet Inter.* **4**, 347–352.

VINCENT, H. (1975). Thèse D'Etat, Université de Grenoble.

VINCENT, H. & BERTAUT, E. F. (1973*a*). *J. Phys. Chem. Solids*, **34**, 151–158.

VINCENT, H. & BERTAUT, E. F. (1973*b*). *Fourth International Conference on Solid Compounds of Transition Elements*, Geneva, p. 200.

VINCENT, H. & PERRAULT, G. (1971). *Bull. Soc. Fr. Minér. Crist.* **94**, 551–555.

WENK, H. R. & RAYMOND, K. N. (1973). *Z. Kristallogr.* **137**, 86–105.

ZACHARIASEN, W. H. (1963). *Acta Cryst.* **16**, 1139–1144.